PROCEEDINGS, Twenty-seventh Workshop on Geothermal Reservoir Engineering
Stanford University, Stanford, California, January 28-30, 2002
SGP-TR-171

GRAVITY MODELING OF THE KARAHA - TELAGA BODAS GEOTHERMAL SYSTEM, INDONESIA

A. Tripp[1], J. Moore[2], G. Ussher[3], and J. McCulloch[4]

1. Department of Geology and Geophysics, University of Utah, Salt Lake City, Utah 84112
2. Energy & Geoscience Institute, 423 Wakara Way, Suite 300, Salt Lake City, UT 84108
3. PB Power, GENZL Division, Auckland, New Zealand
4. Coso Operating Company, LLC, Inyokern, CA

actripp@mines.utah.edu

ABSTRACT

The Karaha-Telaga Bodas geothermal system couples spectacular surface manifestations with an extensive geological and geophysical data set. Examination of fluid inclusions and mineral relationships has allowed development of a thermal history for the system. These data suggest that a quartz diorite intrusion encountered in drill samples provides the heat that drives this system. Delineation of the intrusion's geometry, using gravity data, provides a constraint on the deep thermal structure of the system and the basis for future thermal modeling.

The gravity data has a linear expression that extends the length of the field. A large closed anomaly coincides with the Telaga Bodas thermal area. Using a sphere model gives a depth to the center of gravity of approximately 2400 m. The excess mass constraint on the radius (in meters) of the spherical model is $\Delta\rho(R/304.8)^3 = 100$.

The gentle anomaly along the north-south trending volcanic ridge is consistent with a thin sill of quartz diorite with a width of 1600 m, a depth of 2400 m, and with an approximate thickness of 425 m.

INTRODUCTION

a) Area and problem

Karaha-Telaga Bodas is a large, recently discovered geothermal system in western Java. Figure 1 illustrates the location of the major geothermal and volcanic manifestations and the distribution of the wells. The geothermal system lies beneath a volcanic ridge that extends from Kawah Galunggung, an active volcanic vent, to Kawah Karaha, and then trends to the northwest. Drilling to depths of 3 km, combined with geologic, geochemical, and geophysical investigations are providing a comprehensive picture of the geothermal system's characteristics and evolution. The deep drill holes reached temperatures up to 350°C under much of the area, from Telaga-Bodas in the south to Kawah Karaha located 10 km to the north. Several of these wells bottomed in quartz diorite. Petrographic and fluid inclusion studies of samples from the southern and central parts of the field suggest that the system has had a relatively simple thermal history, and that temperatures have never been substantially cooler than they are today (Moore et al., 2002). This suggests that cooling intrusive rocks related to the quartz diorite provide the heat that drives the system. Figure 2 depicts the current conceptual geological model along the volcanic ridge from Telaga Bodas to the north.

In this paper, we discuss a gravity survey conducted over the geothermal system and use these data to help constrain its deep structure. The fundamental purpose of the analysis is to constrain the geometry of the heat source driving the geothermal system.

b) History of Data

Figure 3 depicts the Bouguer gravity data, as adapted from the original GENZL survey. These data were reduced using a 2.3 g/cc density value for the topography.

A perfunctory examination of this map suggests the presence of an elongated high-density unit, which extends the length of the field from Telaga-Bodas to Kawah Karaha. At Telaga-Bodas it culminates in a radially symmetric anomaly. The cause of this extended anomaly

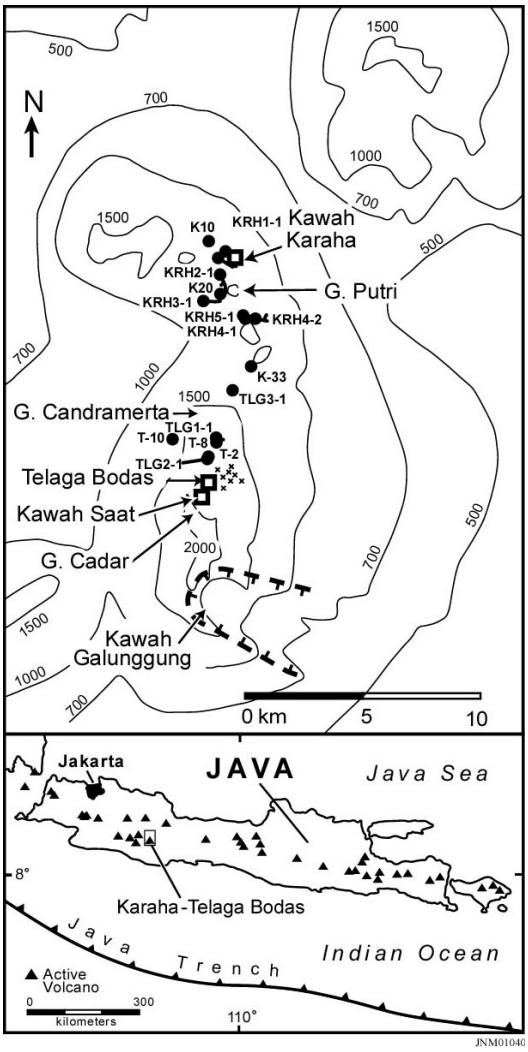

Fig. 1. Map illustrating the distribution of volcanic features, thermal manifestations (Telaga Bodas, Kawah Saat, thermal springs (x's), and Kawah Karaha), and geothermal wells (filled circles) at Karaha-Telaga Bodas. Contour lines show surface elevations (masl). Kawah Galunggung is the main vent of Galunggung Volcano.

could be the quartz diorite at depth. This interpretation is consistent with the high temperatures encountered at relatively shallow depths, high fluid inclusion temperatures, and the presence of secondary minerals (e.g. fluorite, sulfur, tourmaline) suggesting episodic magmatic degassing. Under this interpretation, delineating the gravity source would delineate the heat source for the system. However, the degree of non-uniqueness in gravity interpretations requires a careful approach to achieve the objective.

ROCK DENSITY ANALYSIS

A geometric description of a feature at depth will be biased by poor estimates of the densities of the representative rocks. For this reason, efforts have been made to make the density contrasts as accurate as possible. For example, a cursory examination of the gravity map of Figure 3 might suggest that there is a strong correlation between the topography and gravity data, which would indicate that: 1) there was also a strong correlation between the causative formation at depth and the terrain or; 2) the 2.3 g/cc value chosen for the terrain correction was incorrect.

For the present survey, there are four specific sources of information concerning density values at the surface and at depth. These are:

1) Core samples from the Karaha - Telaga Bodas drill holes;

2) Nettleton profiles over the topographic features;

3) Density logs from the geologically analogous Awibengkok area;

and

4) Density information from the geologically analogous Mt. St. Helens area.

We'll discuss each of these in turn below.

a) Karaha - Telaga Bodas Core Samples

Table 1 gives laboratory measured saturated density values for core samples taken from core hole T-8, located near Telaga Bodas. Most of the rocks are propylitically altered and contain epidote, actinolite, and plagioclase. The density values range from 2.37 to 2.61 gm/cc. The mean density is 2.50 gm/cc with a standard deviation of 0.08 gm/cc. These values would be adjusted downward to give a vapor saturated density value.

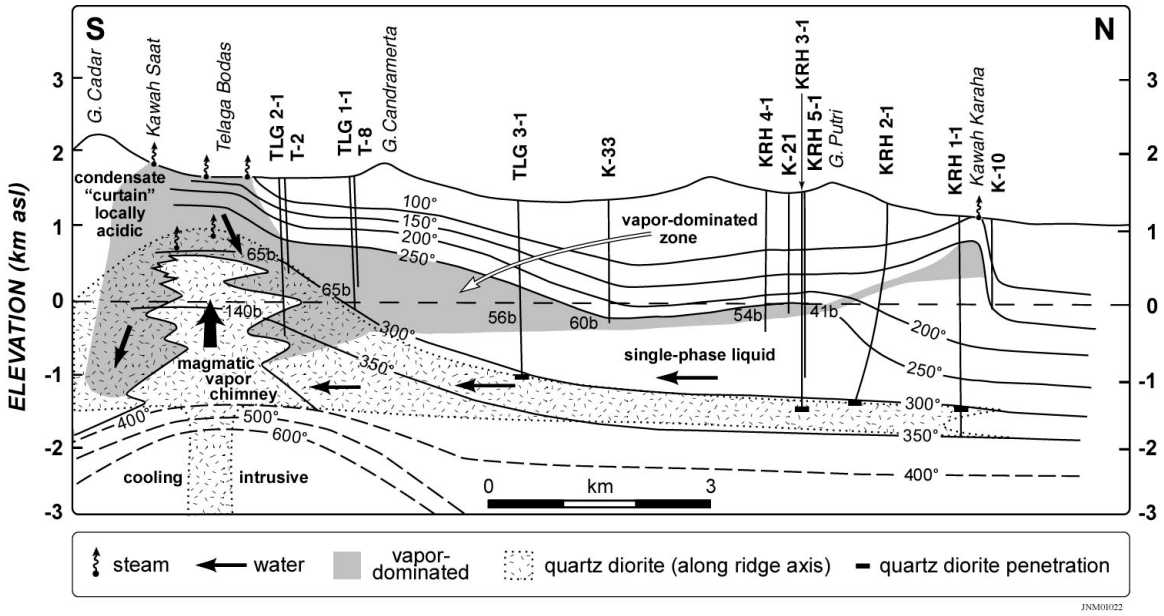

Fig. 2. North-south cross section through the geothermal system. Modified from Allis et al. (2000).

Table 1. Densities of samples from core hole T-8.

Depth of Sample (m)	Sample Lithology	Sample Density (gm/cc)
770.7	andesite lava flow	2.53
778.1	andesite lava flow	2.50
794.7	Tuff	2.57
802.2	Tuff	2.52
885.3	Tuff	2.59
904	Tuff	2.49
978.7	andesite lava flow	2.39
1042	Tuff	2.37
1095.5	Tuff	2.38
1132.3	Tuff	2.61
1174.4	andesite lava flow	2.45
1240.4	andesite lava flow	2.60
1306	Tuff	2.44
	Average	2.50
	Standard Deviation	0.08

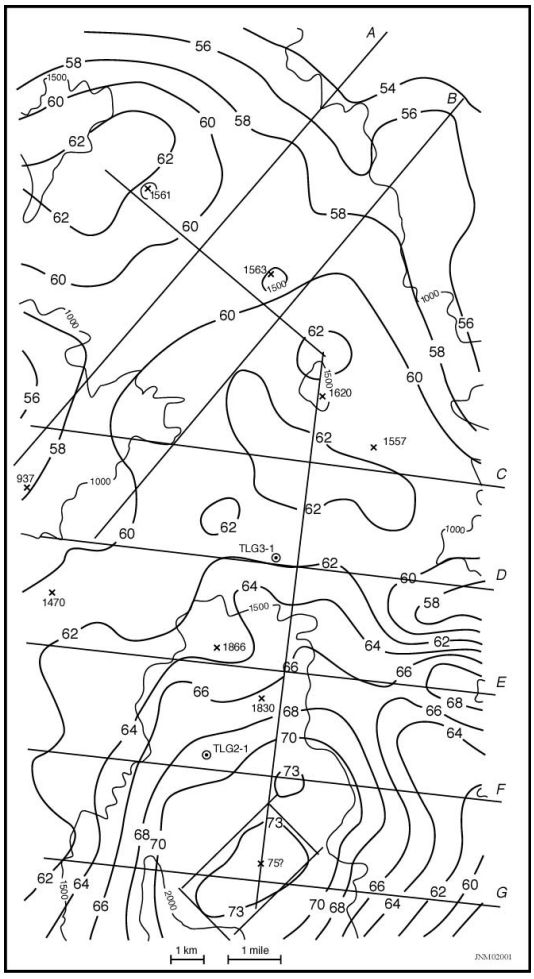

Fig. 3. Map showing Bouguer gravity data.

b) Nettleton Profiles

One means of determining the appropriateness of a terrain correction density is to run small scale gravity profiles over small topographic features and then calculate the correlation between gravity and topographic elevation (Nettleton, 1939, 1940). Unfortunately, the present survey did not measure any such small scale transects. However, it is possible to configure the gravity data into a series of large transects and evaluate the subsequent correlation coefficients.

Figure 3 illustrates a series of transects, labeled A through G, which are oriented approximately perpendicular to the trend of the topography and the data. The data along these transects are modeled below. The correlation between elevation and gravity for all the data point profiles is .61. Assuming that the gravity data and the topography are normally distributed, which is not a very good assumption, a t-test (van der Waerden, 1969) gives a 99% level of significance to this correlation. That is, the topography and the gravity anomalies are not independent. The correlation changes markedly for sub-sets of the data. For example, the correlation coefficient for transect G is -.507, a reversal in sign.

c) Awibengkok Density Logs

Table 2, gives the densities taken from BHI density logs from Awibengkok AWI 1-2 as a function of lithology. Trend analysis of the data indicates that the densities range from approximately 2.68 gm/cc at 1800 m to approximately 2.45 gm/cc at 800 m (Fig. 4). Choosing an extrapolant to a shallower depth is difficult. However, because the polynomial fit to the data flattens at the shallower depths, using it would suggest a near-surface density of approximately 2.45 gm/cc. A linear extrapolation would give a linear gradient of approximately .35 gm/cc - km. The value at the surface would then be approximately 2.25 gm/cc, which is consistent with the Williams et al. (1987) estimates for Mt. St. Helens, given below. The scatter in the data suggests that extrapolation might be a noisy process.

d) Mt. St. Helen's Density Values

Williams et al. (1987) have conducted an extensive study of the density of the geologically analogous Mt. St. Helen's area. On the basis of their investigations at Mt. St. Helens, and at other sites in the Cascades, they suggest a terrain correction value of approximately 2.15 gm/cc.
No sample of quartz diorite was tested in any of the reported studies. Olhoeft and Johnson (1989), on the basis of 33 quartz diorite samples, give a dry bulk density of 2.77 gm/cc with a standard deviation of .15. The mode for this collection is 2.85 gm/cc.

The data above is ambiguous regarding the density used for the terrain corrections. Although the density measurements from Karaha-Telaga Bodas and Awibengkok might suggest that a slightly higher density be used, Nettleton anomaly-elevation correlation changes

Table 2. Densities of samples from Awibengkok. Data from Unocal (1997).

Sample Lithology	Density (gm/cc)	Sample Lithology	Density (gm/cc)
Lahar	2.50	porphyritic andesite breccia	2.61
porphyritic andesite	2.65	weakly welded ash flow tuff	2.67
porphyritic andesite breccia	2.40	andesite or dacitic ash flow	2.31
fallout tuff	2.61	porphyritic andesite flow	2.62
porphyritic pyroxene andesite	2.74	turbidite	2.39
hydrothermal breccia	2.47	Felsic to intermediate welded	2.52
basaltic or basaltic andesite	2.39	felsic tuff	2.52
porphyritic andesite breccia	2.45	basaltic andesite breccia	2.44
non-welded ashflow tuff	2.63	Pumice	2.53
andesite breccia	2.53	fallout vitric ash	2.69
tuffaceous basaltic andesite	2.49	amygdaloidal andesite	2.70
basalt or basaltic andesite	2.35	vitric-lithic tuff	2.67
basaltic andesite	2.58	tuffaceous mudstone	2.37
welded ash flow tuff	2.59	vitric tuff	2.46
ash flow tuff	2.61	lahar breccia with tuff	2.39
Andesite	2.67	vitric fine ash tuff	2.70
		vitric ash tuff	2.79
Average	2.54		
Standard Deviation	0.11		

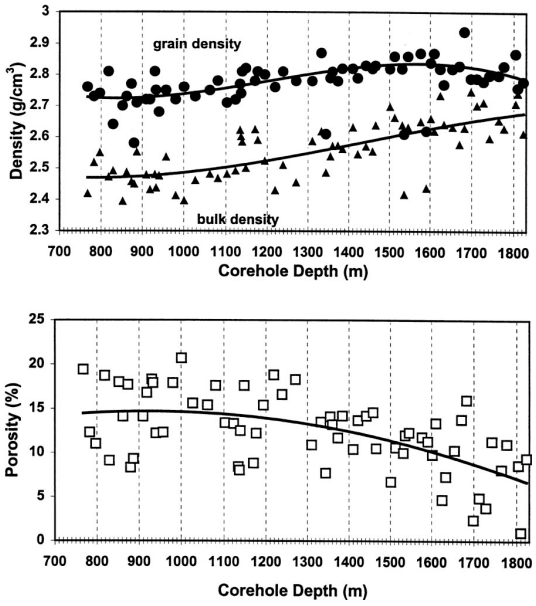

Fig. 4. Bulk densities, grain densities, and porosities as a function of depth fro samples from Awibengkok AWI1-2 (from Unocal, 1997).

for all the transverses depicted suggest that structural changes cannot be corrected with a "one density fits all" topographic correction. The Mt. St. Helen's study suggests that a smaller density value be used. Since the present density value for the terrain corrections is bracketed by the measurements, it will serve for present purposes.

MODELING - ANALYTIC EXPRESSIONS

Given the non-uniqueness present in the gravity responses, simple analytic models are often preferable to extensive computer modeling since the ambiguity in the interpretation can be expressed in a comprehensive form. Here we reference a few expressions that are useful in modeling the gravity response of our area.

If there is a significant strike extent, 2D models are appropriate. Nettleton (1940) gives the gravity response in milligals of a cylinder of radius R as

$$g_z = 12.77\rho\left(R^2 z / (z^2 + x^2)\right)$$

In this equation, the depth of burial of the center of the cylinder is z, ρ is the density contrast in gm/cc, and all dimensions are in kilofeet.

Modeling of closed 3D bodies can be done using the technique suggested by Barnett (1976). However, the amount of non-uniqueness to be

expected in such modeling is large. For this reason, and because of the symmetric nature of the "bulls-eye" anomalies encountered in the gravity map, we have confined our 3D modeling to sphere and ellipsoid models.

The gravity response of a sphere of radius R is given in milligals by Nettleton (1940) as:

$$g_z = 8.53\rho \left[R^3 z / (z^2 + x^2 + y^2)^{3/2} \right]$$

Here the depth of burial of the center of the sphere is z, ρ is the density contrast in gm/cc, and all dimensions are in kilofeet.

The depth of the center of the sphere is easily estimated by the half-width formula

$$z_c = 1.305 x_{1/2}$$

where $x_{1/2}$ is the half-width of the anomaly.

Grant and West (1965) give an approximate formula for the potential U of a triaxial ellipsoid of semi-axis dimensions a,b,c and centered at the origin as

$$-U(x,y,z) = B_{00} / r + B_{02} (3z^2 -- r^2) / 2r^5 + 3 B_{22} (x^2 - y^2) / r^5$$

where

$$B_{00} = 4\pi\rho G abc / 3$$

$$B_{02} = B_{00} (2c^2 - a^2 - b^2) / 10$$

and

$$B_{22} = B_{00} (a^2 - b^2) / 20$$

The first term of this expansion is that of a sphere of equal mass, while the second and third terms are correction terms.

FIELD DATA MODELS

Since the Telaga Bodas anomaly is most significant, we begin with it. To demonstrate the need for a 3D interpretation, we began with a Talwani 2D method, as often used in modeling gravity data. Figure 5 illustrates a model and the data match for transect G for a 2D model generated using the algorithm Grav2D. Although the match to the data is fair, the gravity data in the area is radially symmetric and as such cannot be consistently approximated with a 2D model. This is reflected in the 2D model, whose cross-sectional geometry is perhaps not what one would expect of an intrusive.

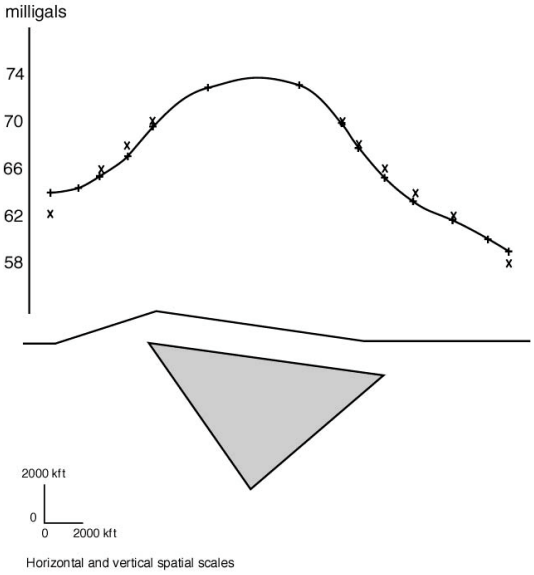

Fig. 5. 2-D density model and model residuals from Talwani modeling of the data along traverse G. The density contrast is .45 gm/cc. The data is given by x's, while the model response is interpolated by the solid line. Vertical and horizontal dimensions are given in kilofeet.

Figure 6 illustrates the match obtained modeling the transect G with a sphere model. One parameter that is uniquely determined in this exercise is $\Delta\rho R^3$, which is proportional to the excess mass of the body and is approximately 100, where R is measured in kilofeet. Another unique parameter is the depth to the sphere center, which is z_c = 7.83 kft.

The asymmetry of the contours suggests that an ellipsoid would be more appropriate than a sphere. However, we can immediately constrain some of the parameters by considering the nature of the anomaly. Since the dominant term of the ellipsoid response gives the response of a spherical source with a volume equal to that of

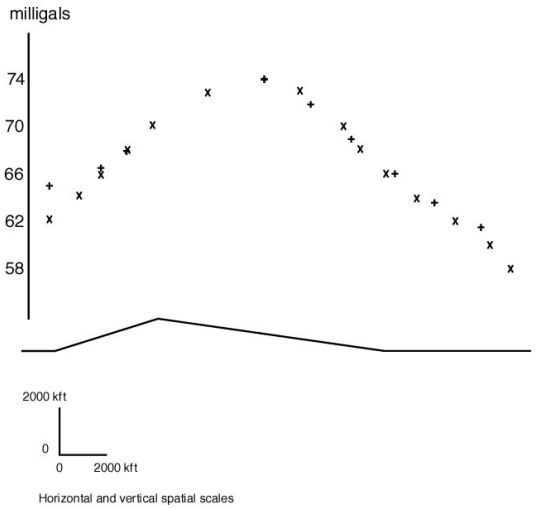

Fig. 6. Modeling data match for sphere along traverse G. The field data are denoted by x's, while the theoretical values are given by +'s. The topography is shown with vertical and horizontal scales equal.

the ellipsoid and centered at the coordinate axis, an ellipsoid matching the anomaly will have a volume close to that of the sphere. Thus, abc=100/ $\Delta\rho$, where $\Delta\rho$ is the density contrast of anomalous body in gm/cc and the linear dimensions are in kilofeet .

Noting the asymmetry in the contours can tighten this constraint. If we assume from the asymmetry that b=2a, then we get the constraint $a^2c\Delta\rho = 50$. This equation can control parametric modeling of the Karaha-Telaga Bodas anomaly. However, it would be nice to find other means of constraining the interpretation.

If we let $\Delta\rho$ =.55 gm/cc, which is the difference between the assumed background density of 2.30 gm/cc and the quartz diorite estimated density of 2.85 gm/cc, the spherical radius is approximately 1.7 km. Drill hole TLG 2-1, which is approximately 1.8 km away from the center of the modeled sphere did not intersect the intrusion. This is consistent with the interpretation.

To the north of the circular - elliptic anomaly is a transition zone leading to a subtle stripe anomaly along the ridge axis. Drill holes along the ridge encountered quartz diorite at depth. What is the relationship of this material to that of the Telaga Bodas anomaly?

One hypothesis is that quartz diorite underlies the entire map area and that the anomalies represent situations in which it approaches close to the surface in a continuous fashion. A major problem with this hypothesis is that extensive high-temperature hydrothermal alteration, which would be present with such a regional feature, is not found in the area. The ridge system anomaly is also small compared to what would be necessary if quartz diorite were present to depth.

An alternate hypothesis is that the quartz diorite thins away from Telaga Bodas. The transition zone between the Telaga Bodas anomaly and the remainder of the anomaly has relatively sharp boundaries to the east and west. This suggests a wedge-shaped zone that "feeds" the intrusive beneath the ridge. Interestingly, the depth of intersection of the quartz diorite in TLG 3-1 is approximately the depth of the center of mass of the Telaga Bodas spherical model.

The ridge anomaly is very small - 2 milligals or so. Modeling the intrusive beneath the ridge as an extended cylinder gives a depth to the center of mass of approximately 1100 m. This is inconsistent with the measured depths to the quartz diorite. An alternate hypothesis is that the north-south anomaly is due to a thin sill underlying the ridge and originating with the wedge-shaped transition zone near Telaga Bodas. Some constraints on the geometry of such a sill can be found using the expression for the response of an " infinite stripe anticline" found in Grant and West (p. 295). Here the maximum gravity anomaly $\Delta g_{max} = 4G\Delta\rho\ t\ \tan^{-1}(w/h)$, where h is the depth of burial, t is the thickness, and 2w is the width of the stripe. With Δg_{max} = 2 milligals, h= 2400 m, and $\Delta\rho$ = .55 gm/cc,

$$t\ \tan^{-1}(w/2400) = 136\ m$$

For example, if we assume, based on the contours in the vicinity of TLG 3-1, that

$w \approx 792m$, we get $t \approx 427$ m.

This sill seems to pinch out as the ridge dog legs to the west. Another radially symmetric anomaly occurs in the northwest part of the map. This time the maximum anomaly value is modest.

OTHER GEOPHYSICAL CONSTRAINTS

In our interpretation, we have emphasized models that give some indication of the

uncertainty inherent in the gravity interpretation. This is not altogether satisfactory, since we wish to find a unique interpretation corresponding to "reality". We also are cognizant that our basic approach must be verified. Both problems are addressed by incorporating constraints from other geophysical data.

a) Resistivity and MT

The resistivity and MT data, as discussed by Iman et al. (2002), is consistent with a thin near-surface conductor in the vicinity of Telaga-Bodas that thickens and deepens laterally. This is consistent with the notion that a heat source is under Telaga-Bodas. High heat flow gives low conductivity alteration, while lower heat flow and descending acidic steam condensate on the flanks of the thermal region give an alteration sequence with a high associated conductivity. The material giving the high heat flow would be our quartz diorite, which in turn would cause the gravity anomaly in the area. Thus the electrical data supports the concept of a localized cooling intrusive in the vicinity of Telaga- Bodas.

b) Temperature Perturbation Estimates

If we assume that the reservoir at depth is ductile, heat flow from the cooling bodies would be predominantly conductive. This means that we could use thermal diffusion models to link heat (and gravity), given suitable estimates of the thermal properties of the intrusive and host rock.

Simple expressions for the temperature diffusion in the vicinity of a cooling sphere or plate, for example, are given in Buntebarth (1984), together with rock thermal property data. Since the intrusive bodies are deep, the effect of the earth's surface should be minor. For more complicated geometries a finite difference approach is advisable.

CONCLUSIONS AND RECOMMENDATIONS FOR FUTURE WORK

Analysis of the Karaha-Telaga Bodas gravity data using simple models yields a self-consistent model of a mushroom-shaped intrusion that reaches relatively shallow depths beneath the thermal area at Telaga Bodas system. The intrusion extends for approximately 10 km to the north as a relatively thin sill that underlies much of the geothermal prospect. Petrologic data suggests that the intrusion is the likely heat source for the geothermal system.

More extensive modeling is desirable. However, due to the intrinsic ambiguity of gravity data, strong constraints would need to be used to justify such modeling. An intriguing possibility is to integrate the thermal history of the system, based on fluid inclusion measurements with the gravity data. Such a venture will require coupling of 3D gravity and thermal diffusion algorithms.

ACKNOWLEDGEMENTS

Funding for AT and JM was provided under DOE contract DE-PS07-98ID13589. The authors would like to thank the management and staff of Karaha Bodas Company, LLC for generously providing the samples and data. The figures were drafted by Doug Jensen.

REFERENCES

Allis, R., Moore, J., McCulloch, J., Petty, S., and DeRocher, T. (2000), "Karaha-Telaga Bodas, Indonesia: a partially vapor-dominated geothermal system," GRC Transactions, 24, 217-222.

Barnett, C.T. (1976), "Theoretical modeling of the magnetic and gravitational fields of an arbitrarily shaped three-dimensional body," *Geophysics*, **41**, no. 6, 1353-1364.

Buntebarth, G. (1984), "Geothermics: An Introduction," Springer-Verlag.

Grant, F.S. and West, G.F. (1965), "Interpretation Theory in Applied Geophysics," McGraw- Hill Book Co.

Raharjo, I., Wannamaker, P., Allis, R. and Chapman, D. (2002), "Magnetotelluric intrepretation of the Karaha geothermal field Indonesia," 27th *Workshop on Geothermal Reservoir Engineering, Stanford University,* in press.

Moore, J. N., Allis, R., Renner, J. L., Mildenhall, D., McCulloch, J. (2002), "Petrologic evidence for boiling to dryness in the Karaha-Telaga Bodas geothermal system, Indonesia," *27th Workshop on Geothermal Reservoir Engineering, Stanford University,* in press.

Nettleton, L. (1939), "Determination of density for reduction of gravimetric observations," *Geophysics*, **4**, 176-183.

Nettleton, L. (1940), "Geophysical Prospecting for Oil," McGraw-Hill Book Co.

Olhoeft, G.R. and Johnson, G.R. (1989), "Densities of rocks and minerals" *in* R.S. Charmichael, ed., *Practical Handbook of Physical Properties of Rocks and Minerals*, CRC Press, Inc. Boca Raton, Florida.

Unocal (1997), "Awibengkok 1-2 Corehole Data Volume, Awibengkok Geothermal Field, West Java, Indonesia," Supplied by Unocal Geothermal Operations to the Energy & Geoscience Institute, University of Utah, July 5, 1997.

Van Der Waerden, B.L. (1969) "Mathematical Statistics," Springer-Verlag, New York.

Williams, D.L., Abrams, G.A., Finn, C., Dzurisin, D., Johnson, D.J., and Derlinger, R.P. (1987), "Evidence from gravity data for an intrusive complex beneath Mt. St. Helens," *Journal of Geophysical Research, B, Solid Earth and Planets*, **92**, no. 10, 10207-10222.